THE ARCHIVE OF MECHANICAL ENGINEERING

Vol. LI 2004 Number 2

Key words: *torsion damper, structural friction, passive and active damping, piezoelectric effect, actuator, sensor*

*ZBIGNIEW SKUP**)

DAMPING OF VIBRATIONS THROUGH TORSION DAMPER DURING STARTING POWER TRANSMISSION SYSTEM

This paper presents a study of the damping of nonlinear vibrations in a two-mass model of mechanical system containing a torsion damper. The starting of the system by harmonic excitation is considered on the assumption of uniformly varying frequency and constant amplitude of the forced moment. Simultaneous structural friction phenomena (passive damping) and piezoelectric effect (active damping) have been considered as well. The problem is considered on the assumption of a uniform unit pressure distribution between the contacting surfaces of friction discs and plunger. The aim of the analysis is to asses the influence of angular acceleration, unitary pressure, external load and electric parameters on the resonance curves of the starting vibrations. The equations of motion of the tested system were solved by means of the Krylov–Bogolubov–Mitropolski method and digital simulation method.

1. Introduction

Due to the complexity of problems with structural friction in mechanical systems, one should take certain simplifying assumptions concerning the friction model were taken. The elastic strain of discs and a plunger as well as influence of piezoelectric effect on damping of vibration in the tested system were take into account. The author based his considerations on previously derived physical connections for frictional torsion damper. In the design process of power transmission system and selection of existing models of dampers, basic standard calculation methods were applied. It is essential, however, to take account of a natural source of vibration damping by means of

*) *The Institute of Machine Design Fundamentals, Warsaw University of Technology; Narbutta 84, 02-524 Warsaw, Poland; E-mail: Zbigniew.Skup@ipbm.simr.pw.edu.pl*

structural friction and piezoelectric effect. Developments in new materials have made it possible to create the so called "intelligent" materials [electrorheological (ER) fluid and magneto-rheological (MR) fluid, alloys with shape memory, piezoelectric polymers]. FR and MR fluids are multi-phase materials consisting of a dispersion of polarizable particles of oil, they exhibit properties typical of a viscoelastic material. These materials change their properties under the influence of magnetic and electric field, temperature or mechanical stresses.

The basic electromechanical properties of piezoelectric material – lead zirconate titanate (PZT) are presented in the paper in terms of their capacity to damp torsion vibrations in the mechanical system considered. Piezoceramics exhibit natural shear effect that is three times stronger than the longitudinal one. This phenomenon can be successfully utilised in torsion systems for vibration control, as piezoceramics constitute perfect elements for actuator applications. Active control is achieved through a closed loop with proportional feedback (proportional – plus – derivative controller).

Meng – Kao Yeh and Chih – Yuan Chin [5] proved the applicability of piezoelectric sensors for measuring torsional vibration of shafts. Introductory theoretical studies of shafts vibration inducted by piezoelements based on PZT ceramics were presented by the authors of works [3] and [10]. Experimental investigations dealing with actively controlled torsion system were carried out by Chia -Chi Sung et al. [1].

2. Equations of motion

We will assume a two – mass model of the mechanical system which contains a frictional torsion damper as represented in Figure 1. Structural friction occurs between cooperating surfaces of discs 2 and plunger 1. Discs 2 are pressed down to plunger 1 by means of springs 3. The shaft is equipped with two piezoelectric elements: actuator 4 and sensor 5. The actuator is posed by a ring – shaped element of considerable thickness, thus, its moment of inertia must be taken into account. The sensor may be made of PZT or PVDF (piezoelectric foil) yet it must be thin enough to be neglected in total inertia balance of the system. The actuator and the sensor are electronically coupled with proportional feedback ruling the performance of the arranged control system.

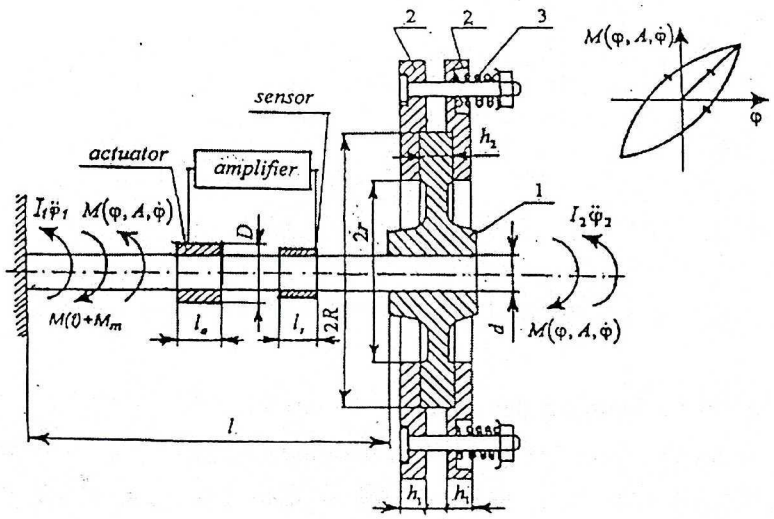

Fig. 1. Physical model of the considered friction torsion damper

Equations of motion of the considered system may be written as follows:

$$I_1 \ddot{\varphi}_1 + M(\varphi, A, \dot{\varphi}) = M_m + M(t) + M_a$$
$$I_2 \ddot{\varphi}_2 - M(\varphi, A, \dot{\varphi}) = 0. \tag{1}$$

where: φ_1, φ_2 – angles of torsion of plunger and discs damper; φ, A – relative angular displacement of discs and plunger and its vibration amplitude; I_1, I_2 – reduced moment of inertia of the movable parts of the engine, actuator, plunger and of discs, springs, screws in the damper (reduction to the axis of damper); $M(\varphi, A, \dot{\varphi})$ – damper moment of friction in a cycle represented by structural hysteresis loop (Fig. 1), dependent on the relative displacement, amplitude and its sign of velocity; M_a – torsional moment generation by actuator; $M(t) + M_m$ – variable engine torque described by a constant average value M_m and a discrete forcing torque $M(t)$ in the form of harmonic excitation with uniformly varying frequency and constant amplitude as in [2], [6], [13], [14]. Therefore $M(t)$ takes the following form:

$$M(t) = M_0 \sin\theta, \quad \theta = \frac{\varepsilon t^2}{2} + \varphi_0, \quad \omega(t) = \frac{d\theta}{dt} = \varepsilon t, \tag{2}$$

where: M_0 – forced torque amplitude; θ – phase angle; φ_0 – phase displacement angle; ε – angular acceleration; $\omega(t)$ – excitation frequency; t – time.

3. Determination of moment of friction

According to the studies presented in works [11] and [12], the relationship between angular displacement and moment of friction is as follows:

$$\varphi_{n+1}(M)=\varphi_n(M_n)+\frac{(M-M_n)l}{GI_0}+\kappa\left\{6+\nu(M-M_n)sign\frac{dM}{dt}-\Omega\right\}sign\frac{dM}{dt}, \quad (3)$$

where

$$\nu=\frac{3}{2\pi p\mu R^3}, \quad \kappa=\frac{2\beta(k_1+k_2)}{k_1k_2}, \quad \beta=\frac{p\mu R}{6}, \quad k_1=Gh_1, \quad k_2=Gh_2,$$
$$I_0=\frac{\pi d^4}{32}, \quad \Omega=6\left[1+\frac{\nu}{2}(M-M_n)sign\frac{dM}{dt}\right]^{1/3} \quad (4)$$

notations: $\varphi_n(M_n)$, $\varphi_{n+1}(M)$ – the maximum angular displacement in n^{th} and $(n+1)^{th}$ vibration half – period; $(M-M_n)$ – increase in load in the $(n+1)^{th}$ stage of motion vs. n^{th} stage of motion; k_1, k_2, h_1, h_2 – discs and plunger stiffness and their thicknesses; μ – friction coefficient; p – pressure per unit area (unitary pressure); R – external radius of the discs; G – shear moduli; I_0 – cross-sectional moment of inertia of the shaft.

Since in real design friction dampers we have $\frac{\nu}{2}(M-M_n) \ll 1$, the expression with powers 1/3 in Eqn. (4) can be expanded into power series. Neglecting the terms of orders higher than 3, we obtain

$$\varphi_{n+1}(M)=\varphi_n(M_n)+\frac{(M-M_n)l}{GI_0}+\frac{\kappa\nu^2}{6}(M-M_n)^2sign\frac{dM}{dt} \quad (5)$$

Expression (5) can be now easily reversed to obtain the hysteresis loop in terms of the moment of friction as a function of relative angular displacement:

$$M-M_n=k\left\{\frac{2}{\kappa_1}sign\frac{d\varphi}{dt}\left(-1\pm\left[1+\kappa_1(\varphi-\varphi_n)sign\frac{d\varphi}{dt}\right]^{1/2}\right)\right\}, \quad (6)$$

where

$$k = \frac{GI_0}{l}, \qquad \kappa_1 = \frac{G^2 I_0^2 (k_1 + k_2)}{2\pi^2 l^2 k_1 k_2 p \mu R^5} \tag{7}$$

where k denotes the stiffness of the elastic shaft of length l and diameter d, κ_1 is a nondimensional parameter.

The solution with a minus sign before root must be rejected because it would not be justified from the physical point of view. For the relationship (6), in every stage of motion, it is necessary to take new initial conditions. The problem can be eliminated if the coordinate system is moved to the centre of the hysteresis loop. The change of coordinates of the system has been performed on the basis of [7] and [9].

After transformations, the result can be written as

$$M(\varphi, A, \dot{\varphi}) = \frac{k}{\kappa_1} sign\,\dot{\varphi} \left\{ 2[1 + \kappa_1 (\varphi - A)\, sign\,\dot{\varphi}]^{1/2} - \right.$$
$$\left. - 1 - (1 - 2\kappa_1 A sign\,\dot{\varphi})^{1/2} \right\} \tag{8}$$

4. Torque generated by the actuator

By applying the ring – type actuator (terminology after Chia-Chi Sung et al. [1]), one can derive from a version of constitutive equation the following formula, henceforth called the actuator law:

$$\tau_a = \frac{2G_a d_{15}^a U_a}{l_a} \tag{9}$$

where: τ_a, G_a – shear stress and shear modulus of PZT material (for actuator); l_a – width of the actuator; U_a – applied voltage actuator; d_{15}^a – electromechanical coupling constant actuator.

The torsion moment M_a produced by the actuator can be calculated by integrating the shear stress τ_a over the entire cross-section of the piezoelement:

$$M_a = \int_{d/2}^{D/2} \tau_a \rho\, dF \tag{10}$$

where: d, D – inner and outer actuator diameter; $dF = 2\pi\rho d\rho$ – elementary sensor area.

Active interaction between the actuator and sensor performance is secured by the control law:

$$U_a = k_p U_s \tag{11}$$

where U_s is voltage produced by the sensor; k_p are the gain factor introduced by the electronic circuit.

Lee [4] and Tzou [15] came up with the reasoning to determine the amount of electric charge generated by the sensor. Classical formula for flat condensers makes it possible to find the voltage swept by the sensor. The final result can be written as:

$$U_s = \frac{G_s d_{15}^s d\varphi_s}{2\varepsilon_0 \varepsilon_s}, \qquad \varphi_s = \frac{M_1(\varphi, A, \dot{\varphi}) l_s}{GI_0} \tag{12}$$

where: ε_0, ε_s are the absolute and relative dielectric permittivity of sensor respectively, $M_1(\varphi, A, \dot{\varphi})$ – torque moment transmited by sensor; G_s – shear modulus of sensor material; l_s – width of the sensor; d_{15}^s – coupling constant sensor.

The torque moment $M_1(\varphi, A, \dot{\varphi})$ may be written as follows

$$M_1(\varphi, A, \dot{\varphi}) = M(\varphi = A, A, \dot{\varphi}) = \frac{k}{\kappa_1} sign\dot{\varphi} \left[1 - (1 - 2\kappa_1 A sign\dot{\varphi})^{1/2}\right] \tag{13}$$

Therefore, substituting equations (9), (11), (12) and (13) into equation (10) and rearranging, gives

$$M_a = \kappa_2 sign\dot{\varphi} \left[1 - (1 - 2\kappa_1 \varphi_s sign\dot{\varphi})^{1/2}\right] \tag{14}$$

$$\kappa_2 = \frac{\pi G_a G_s d_{15}^a l_s d (D^3 - d^3) k_p k}{12 G l_a I_0 \kappa_1 \varepsilon_0 \varepsilon_s} \tag{15}$$

5. Solution of equation of motion

After introducting the relative angular displacement to equations of motion (1)

$$\varphi = \varphi_1 - \varphi_2, \tag{16}$$

as well as the reduced moment of inertia

$$I_z = \frac{I_1 I_2}{I_1 + I_2}, \qquad I = \frac{I_z}{I_1} \tag{17}$$

and applying (8) we can rearrange equations of motion (1) into the following form:

$$I_z \ddot{\varphi} + M(\varphi, A, \dot{\varphi}) = \frac{k}{\kappa_1} sign\dot{\varphi} \{2[1 + \kappa_1(\varphi - A)sign\dot{\varphi}]^{1/2} - \\ - 1 - (1 - 2\kappa_1 A sign\dot{\varphi})^{1/2}\} = \Psi, \tag{18}$$

$$\Psi = I[M(t) + M_m + M_a] \tag{19}$$

In order to apply the asymptotic Krylov – Bogolubov – Mitropolski method, we have to expand the square root in (18) in to a power series first. As a result of the analysis and numerical calculations, it was established that values of the root and the sum of the first five terms of the series are very close to each other. The rest of convergent series taken from sixth term quickly tends to zero with increasing number of thrown awuy terms.

Thus, after some transformations equation of motion (18) takes the following form:

$$I_z \ddot{\varphi} + k_z \varphi = \nu_1 F(\varphi, A, \dot{\varphi}) + IM_0 \sin\left(\frac{\varepsilon t^2}{2} + \varphi_0\right), \tag{20}$$

where

$$k_z = \frac{k}{\sqrt{1 + \kappa_1 A}}. \tag{21}$$

$$\nu_1 F(\varphi, A, \dot{\varphi}) = \frac{k}{\kappa_1} sign\dot{\varphi} \{1 + (1 - 2\kappa_1 A sign\dot{\varphi})^{1/2} - \\ 2\Gamma[1 - \kappa_1 A sign\dot{\varphi}]^{1/2}\} + I[M_m + M_a], \tag{22}$$

$$\Gamma = 1 - \frac{\kappa_1^2 \varphi^2}{8(1 - \kappa_1 A sign\dot{\varphi})^2} + \frac{\kappa_1^3 \varphi^3 sign\dot{\varphi}}{16(1 - \kappa_1 A sign\dot{\varphi})^3} - \\ - \frac{5\kappa_1^4 \varphi^4}{128(1 - \kappa_1 A sign\dot{\varphi})^4} \tag{23}$$

where ν_1 denotes small dimensionless parameter and k_z – torsional stiffnes of the system. The solution of non-linear differential equation describing non-stationary motion of the system is assumed in the first approximation as

$$\varphi = A\, cos(\theta + \xi) \tag{24}$$

By incorporating the asymptotic method [6] and [8], we can obtain the equations describing the amplitude of the angular displacement A and the phase shift ξ as given below:

$$\frac{dA}{dt} = \nu_1 A_1(t, A, \xi), \tag{25}$$

$$\frac{d\xi}{dt} = \omega_0 - \omega(t) + \nu_1 B_1(t, A, \xi). \tag{26}$$

where

$$\omega_0 = \sqrt{\frac{k_z}{I_z}} - \text{natural frequency of the system} \tag{27}$$

After double differentiating equation (24) and substituting (24) and (27) to the left side of the equation of motion (20), we get

$$I_z \ddot{\varphi} + k_z \varphi = \nu_1 I_z \left[\left\{ [\omega_0 - \omega(t)] \frac{dA_1}{d\xi} - 2A\omega_0 B_1 \right\} \cos(\theta + \xi) - T \right], \tag{28}$$

$$T = \left\{ \left[[\omega_0 - \omega(t)] A \frac{dB_1}{d\xi} + 2\omega_0 A_1 \right] \right\} \sin(\theta + \xi) \tag{29}$$

After averaging the right side of equation (20) during one period time, the following is obtained

$$\nu_1 F(\varphi, A, \dot{\varphi}) + IM_0 \sin\theta = \frac{\nu_1 \cos(\theta + \xi)}{\pi} \int_0^{2\pi} F(\varphi, A, \dot{\varphi}) \cos(\theta + \xi) d(\theta + \xi) +$$

$$+ \frac{\nu_1 \sin(\theta + \xi)}{\pi} \int_0^{2\pi} F(\varphi, A, \dot{\varphi}) \sin(\theta + \xi) d(\theta + \xi) - \qquad (30)$$

$$- IM_0[\cos(\theta + \xi)\sin\xi - \cos\xi \sin(\theta + \xi)$$

After comparison of the right side of equations (28) and (30) standing by the same harmonics and powers ν_1 and after some transformation of the formulae for $A_1(t, A, \xi)$ and $B_1(t, A, \xi)$, we obtain

$$A_1(t, A, \xi) = -\frac{1}{2\pi I_z \omega_0} \int_0^{2\pi} F_0(A, \chi) \sin\chi d\chi - \frac{IM_0 \cos\xi}{\nu I_z[\omega_0 + \omega(t)]}, \qquad (31)$$

$$B_1(t, A, \xi) = -\frac{1}{2\pi I_z \omega_0 A} \int_0^{2\pi} F_0(A, \chi) \cos\chi d\chi + \frac{IM_0 \sin\xi}{\nu I_z A[\omega_0 + \omega(t)]} \qquad (32)$$

where

$$F_0(A, \chi) = F(\varphi, \dot{\varphi}) = F(A\cos\chi, -A\omega_0 \sin\chi), \qquad \chi = \theta + \xi. \qquad (33)$$

Substituting formulae (31) and (32) in to the system of equations (25), (26) and rearranging them, we obtain

$$\frac{dA}{dt} = -\frac{\nu_1}{2\pi I_z \omega_0} \int_0^{2\pi} F_0(A, \chi) \sin\chi d\chi - \frac{M_0 \cos\xi}{I_1[\omega_0 + \omega(t)]}, \qquad (34)$$

$$\frac{d\xi}{dt} = \omega_0 - \omega(t) - \frac{\nu_1}{2\pi I_z \omega_0 A} \int_0^{2\pi} F_0(A, \chi) \cos\chi d\chi + \frac{M_0 \sin\xi}{I_1 A[\omega_0 + \omega(t)]}. \qquad (35)$$

Because of the discontinuity of the function $F_0(A, \chi)$ at $\dot{\varphi} = 0$, we confine the analysis to one half-period of the vibrating motion. The integration interval $(0, 2\pi)$ will be divided in to the following two intervals: $(0, \pi)$ when $sign\dot{\varphi} < 0$ $(A > 0)$, and $(\pi, 2\pi)$ when $sign\dot{\varphi} > 0$ $(A < 0)$.

Equations (34) and (35) can be presented in the form:

$$\frac{dA}{dt} = -h_{eq}(A) A - \frac{M_0 \cos\xi}{I_1[\omega_0 + \omega(t)]}, \qquad (36)$$

$$\frac{d\xi}{dt} = \omega_{0eq}(A) - \omega(t) + \frac{M_0 \sin\xi}{I_1 A[\omega_0 + \omega(t)]}. \tag{37}$$

where $\omega_{0eq}(A)$ denotes equivalent frequency, $h_{eq}(A)$ – equivalent damping coefficient.

These coefficients can be calculated with the help of the formulae included in works [6 – form. 3.53, pp. 91] and [8 – form. 2.150, 2.151, pp. 65]. Therefore

$$h_{eq}(A) = \frac{\nu_1}{2\pi I_z \omega_0 A} \int_0^{2\pi} F_0(A, \chi) \sin\chi d\chi, \tag{38}$$

$$\omega_{0eq}(A) = \omega_0 - \frac{\nu_1}{2\pi I_z \omega_0 A} \int_0^{2\pi} F_0(A, \chi) \cos\chi d\chi \tag{39}$$

After integration, relations for the equivalent damping coefficient (38) and equivalent frequency (39) take the form:

$$h_{eq}(A) = \frac{k}{\pi \kappa_1 \omega_0 I_z A}\left[\frac{\kappa_1}{k}(C + H) - 2\left(1 - \sqrt{B} - \sqrt{E}\right) - \sqrt{A_2} - \sqrt{D} - Y\right], \tag{40}$$

$$\omega_{0eq}(A) = \omega_0 + \frac{3k\kappa_1^2 A^2}{128 I_z \omega_0}\left(B^{-5/2} + E^{-5/2}\right) \tag{41}$$

where

$$A_2 = 1 + 2\kappa_1 A, \quad B = 1 + \kappa_1 A,$$
$$C = I\left\{M_m - \kappa_2\left[1 - (1 + 2\kappa_1 A)^{1/2}\right]\right\}, \quad D = 1 - 2\kappa_1 A, \tag{42}$$

$$E = 1 - \kappa_1 A, \quad H = I\left\{M_m + \kappa_2\left[1 - (1 - 2\kappa_1 A)^{1/2}\right]\right\} \tag{43}$$

$$Y = \frac{\kappa_1^2 A^2}{4}\left[\frac{1}{3}\left(B^{-3/2} + E^{-3/2}\right) + \frac{\kappa_1^2 A^2}{16}\left(B^{-7/2} + E^{-7/2}\right)\right]. \tag{44}$$

Finally, in two basic differential equations (36) and (37) we have the relation for the relative angular displacement amplitude A (vibration amplitude) of discs and plunger as function of the excitation frequency ω (the resonance curves for starting vibrations). The influence of the external load,

unit pressure, geometric parameters, friction coefficient, angular acceleration and the gain factor on resonance curves of the system has been investigated.

6. Numerical results

Differential equations (36) and (37) have been solved by means of the RUNGE-KUTTA method of fourth order with Gill's correction (the program library of PDP RT 11 company, Subroutine RKGS). In order to compare the numerical results, a comparing program has been worked out, using the GEAR method.

Numerical calculations carried out for the above formulae incorporated the following data:
$h_1 = 0.004$ m, $h_2 = 0.010$ m, $R = 0.0585$ m, $\varepsilon = 300$ 1/s^2, $M_0 = 30$ Nm, $\mu = 0.25$, $d = 0.054$ m, $I_1 = 0.03$ kgm^2, $I_2 = 0.04$ kgm^2, $1 = 0.65$ m, $p = 0.8 \cdot 10^5$ N/m^2, $l_a = 0.04$ m, $l_c = 0.04$ m, $G = 8.2 \cdot 10^{10}$ N/m^2, $G_a = 6.3 \cdot 10^9$ N/m^2, $G_s = 2 \cdot 10^9$ N/m^2, $d_{15}^a = 5.6 \cdot 10^{-10}$ m/V – for PZT (type PIC 255), $d_{15}^s = 0.23 \cdot 10^{-10}$ m/V – for PVDF, $\varepsilon_s = 12$, $\varepsilon_0 = 0.088 \cdot 10^{-10}$ F/m, $k_p = 0 \div 1$ (in technical cases the gain factor often takes of values from this range).

The results of numerical calculations are presented in the form of resonance curves in Fig. (2a,b; 3a,b). The analysis of the results of numerical calculations shows that if we take account of structural friction occuring between surfaces of discs friction and plunger and piezoelectric effect, the efficiency of damping is greater. The greater amplifier gain k_p is, the more visible the effect (Fig. 2a).

The influence of the unitary pressure p on the vibration amplitude A of the system in function of the excitation frequency ω is presented in Fig. 2b. It can be seen that greater values of unitary pressure drive vibration amplitudes higher and shift them towards lower values of forced frequency. The reason which causes lower value of the resonant amplitudes of angle displacement with decreasing value of unitary pressure is the decrease of the friction force. This increases the mutual surface zone of sliding discs of damper after plunger. There is a certain optimal value of unitary pressure for which the sliding zone of the contacting elements is the largest. That phenomenon is accompanied by more intensive dissipation of energy, which increases the vibrations damping in the tested system. When unitary pressure is high, the discs can stay put. Then, the system operates as a stiff joint of bodies. There can be no damping of vibrations involved through structural friction. Therefore, resonance curves in the pre-resonance period and especially post-resonance period may differ considerably.

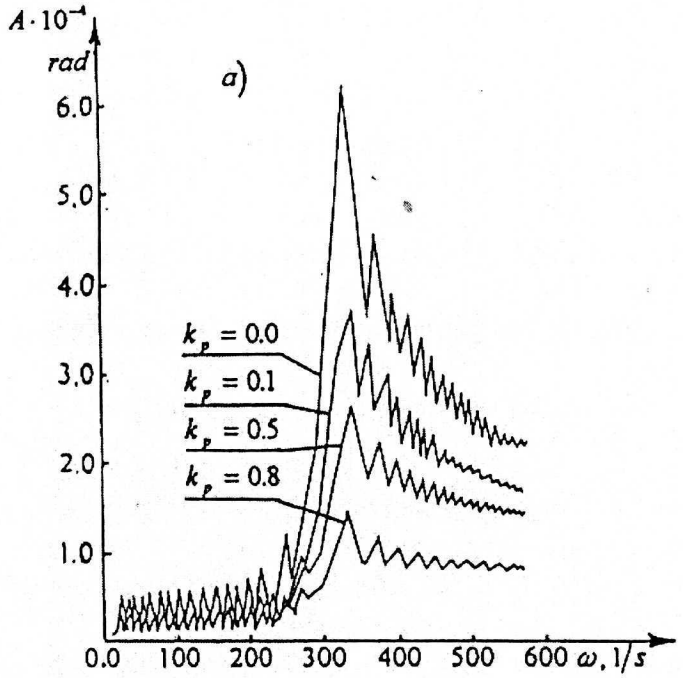

Fig. 2a. Graphs of resonant curves for various values of the gain factor k_p

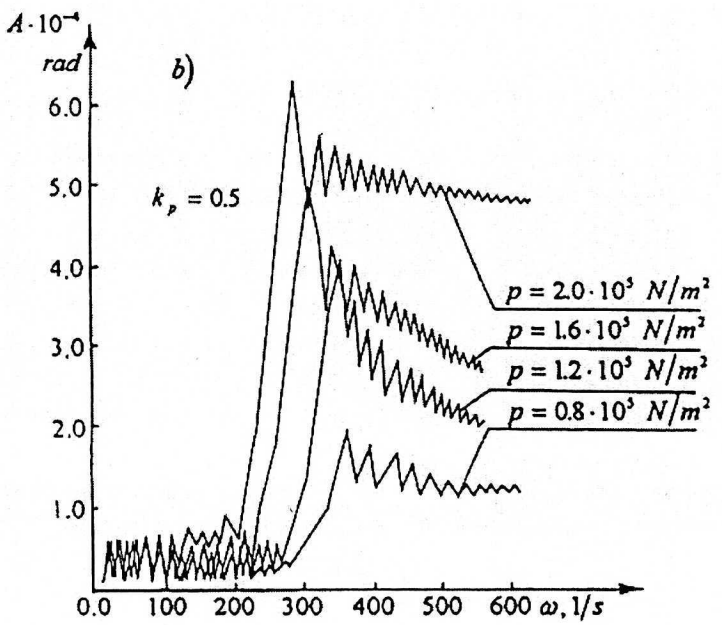

Fig. 2b. Graphs of resonant curves for various values of the unitary pressure p

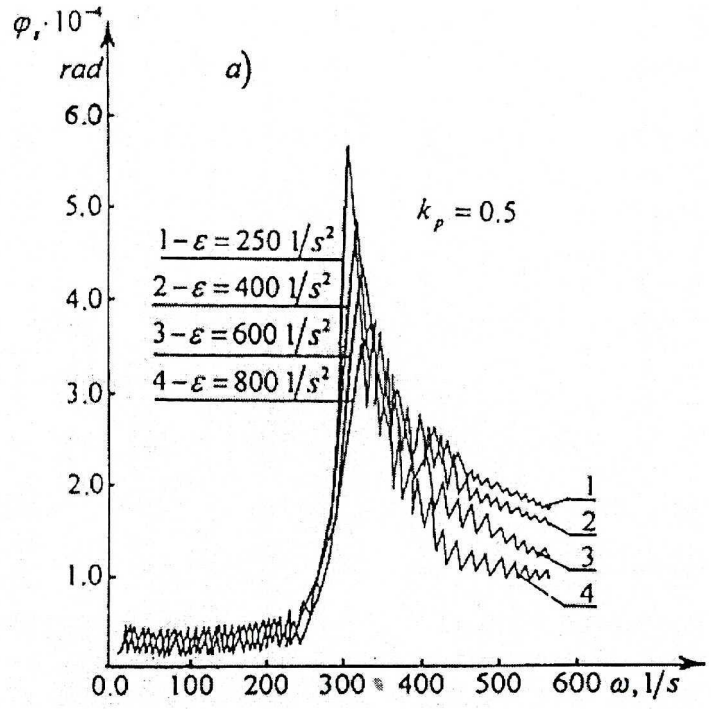

Fig. 3a. Graphs of resonant curves for various values of the angular acceleration ε

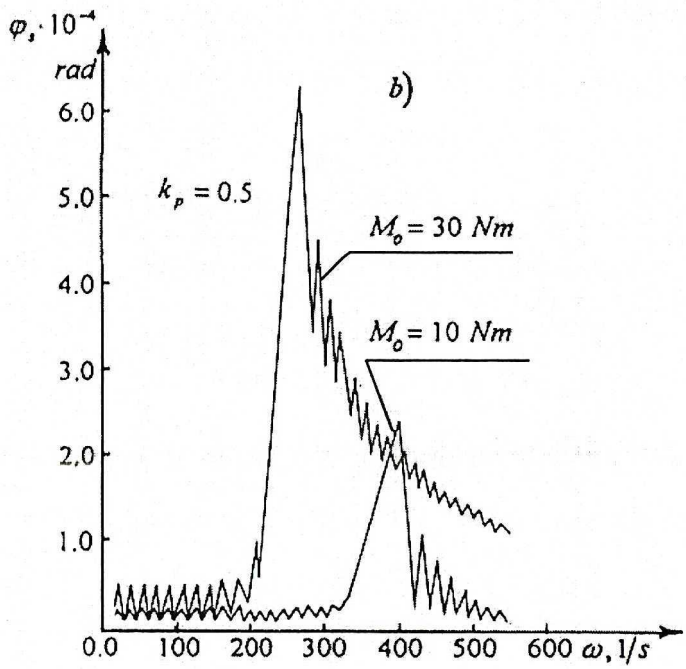

Fig. 3b. Graphs of resonant curves for various values of the forcing torque amplitude M_0

In Fig. 3a, we can see the relation of vibrations' amplitude A versus excitation frequency ω for different angular accelerations. The resonant amplitudes decrease along the increase of the angular acceleration ε. We can also observe the beating phenomenon before and after the resonance. Shifting of resonances towards higher frequencies is brought about by the retardation effect (as mentioned in the previous section).

The influence of the forcing torque amplitude M_0 on the vibration amplitude A in function of excitation frequency ω is shown in Fig. 3b. Increasing value of the forcing torque amplitude leads to a growth in value of the main resonance amplitude.

In the case of quasi-deterministic excitation, the existence of the curves corresponding to a decaying post-resonance (superresonant) vibration confirms the peculiarity of the resonant transition. Resonance amplitudes begin to increase for different values of external load (Fig. 3b) due to a change in the value of the system's natural frequency. Natural frequency depends on the value of the damper moment of friction and, thus, also on the amplitude of the external load [13 – form. 9.12] . Figures (2a,b; 3a,b) reveal oscillating characteristics of the amplitudes. The oscillations vanish outside of the main resonance zone. The singularity of a passage through resonance in the form of fading "beats" has been confirmed as well. This peculiarity was also pointed out in works [2], [6], [13], [14]. During the starting stage, post-resonance (superresonant) amplitudes are greater than pre-resonance (subresonant) ones, and they have an oscillating character. After some time, the phenomenon of "beats" disappears and the amplitude sets on appropriate level value.

7. Concluding remarks

Structural friction between the contacting surfaces of discs and plunger, produces increases in damping of vibrations in the tested system. Higher value of the amplification factor by the electronic circuit increases the intensity of vibration damping. The phenomena properties of piezoelectric material can be utilized in torsion systems for vibration control as piezoceramics constitute perfect elements for actuator applications.

Active control by piezoelectric elements and structural friction proves to be a powerful tool in reducing vibration amplitude of torsional systems. Application of electronic damping gives excellent results, especially in control systems governed by feedback, even for different points of actuator application and spatial sensor/actuator dislocation. This is highly important since real technical conditions may not always allow arbitrary piezoelements application.

The damping effect is the greatest for an appropriate value of the moment of friction, because the zone of relative slip between the damper discs and plunger is the largest. The efficiency of vibration damping by means of a frictional damper is largery influenced by the following factors: forcing torque amplitude, moment of friction (unitary pressure, friction coefficient), angular acceleration, stiffness of the shaft, discs and plunger, gain factor. The effects of structural friction and piezoelectric effect can be used in order to improve the design methods of dynamic systems.

Manuscript received by Editorial Board, April 15, 2002;
final version, July 02, 2004.

REFERENCES

[1] Chia-Chi Sung, Vasundara V. Varadan, Xiao-Qi Bao, Vijay K. Varadan: Active Torsional Vibration Control Experiments Using Shear-Type Piezoceramic Sensors and Actuators, Journal of Intelligent Material Systems and Structures,1994, Vol. 5, No. 3, pp. 436÷442.

[2] Gałkowski Z.: Drgania niestacjonarnego połączenia tuleja-wał z uwzględnieniem tarcia konstrukcyjnego oraz momentów bezwładności połączenia, X Konferencja, Metody i środki projektowania automatycznego, IPBM, Politechnika Warszawska (Vibration of a Non-Stationary Sleeve-Shaft Joint with Structural Friction and Inertia Moment Taken into Consideration, X Conference on Methods and Tools in Automatic Design, Institute of Machine Design Fundamentals, Warsaw University of Technology), 1985, pp. 134÷145.

[3] Kurnik W., Przybyłowicz P.M.: Torsional Vibration of a Tube with Piezoelectric Actuators, Zeitschrift fur Angewandte Matematik und Mechanik, 1995, Vol. 75, No.1, pp. S55÷S56.

[4] Lee C.K.: Theory of Laminated Piezoelectric Plates for the Design of Distributed Sensors/Actuators. Part I: Governing Equations and Reciprocal Relationships, Journal of the Acoustical Society of America, 1990, Vol. 87, No. 3, pp. 1144÷1158.

[5] Meng-Kao Yeh, Chih-Yuan Chin: Dynamic Response of Circular Shaft with Piezoelectric Sensor, Journal of Inteligent Material Systems and Structures, 1994, Vol. 5, No. 6, pp. 833÷840.

[6] Mitropolskij Ju.A.: Probliemy asimptoticzeskoj tieorii niestacjonarnych koliebanii, Izdat. Nauka, Moskwa, 1964.

[7] Osiński Z., Kosior, A.: Wpływ tarcia konstrukcyjnego na krzywe rezonansowe układu przy wymuszeniu harmonicznym, X Konferencja Dynamiki Maszyn, IPBM Politechniki Warszawskiej (The Influence of Structural Friction on Resonance Curves of a System with Harmonic Excitation, X Machine Dynamics Conference, Institute of Machine Design Fundamentals, Warsaw University of Technology), 1976, pp. 185÷195.

[8] Osiński Z.: Teoria Drgań, PWN, Warszawa (Theory of Vibrations, PWN, Warsaw), 1978.

[9] Osiński Z.: Tłumienie drgań mechanicznych, PWN, Warszawa (Damping of Mechanical Vibrations, PWN, Warsaw), 1986.

[10] Przybyłowicz P.M.: Torsional Vibration Control by Active Piezoelectric System, Journal of Theoretical and Applied Mechanics, 1995, Vol. 4, No. 33, pp. 809÷823.

[11] Skup Z.: Analiza tarciowego tłumika drgań skrętnych poddanego równomiernemu i nierównomiernemu rozkładowi nacisków z uwzględnieniem tarcia konstrukcyjnego, Rozprawa doktorska, Politechnika Warszawska (Analysis of a Frictional Torsion Damper Exposed to

Unitary and Non-Unitary Distribution of Pressure with Structural Friction Taken into Consideration, Ph.D. thesis, Warsaw University of Technology), 1976.

[12] Skup Z.: Drgania swobodne układu ze sprzęgłem ciernym przy uwzględnieniu tarcia konstrukcyjnego, AGH, Kraków, Mechanika (Free Vibration of a System with a Friction Clutch with Structural Friction Taken into Account, AGH, Krakow, Mechanics, 1987, Vol. 6, pp. 105÷122), 1987, t. 6, z. 2, str. 105÷122.

[13] Skup Z.: Wpływ tarcia konstrukcyjnego w wielotarczowym sprzgle ciernym na drgania w układzie napędowym, Prace naukowe, Mechanika z. 167, Oficyna Wydawnicza Politechniki Warszawskiej, 1998, (Rozprawa habilitacyjna) (The Influence of Structural Friction in a Multiple-Disk Friction Clutch on Vibration in a Power Transmission System, Scientific Papers, Mechanics, Vol. 167, Oficyna Wydawnicza Warsaw University of Technology, 1998, habilitation thesis).

[14] Tylikowski A.: Drgania układu liniowego wywołane procesem przypadkowym o jednostajnie zmiennej częstości, Rozprawy inżynierskie (Vibration of a Linear System Excited by a Random Process with Steadily Variable Frequency, 1969, Vol. 17, pp. 269÷280), 1969, nr. 17, z. 2, str. 269÷280.

[15] Tzou H.S.: Distributed Piezoelectric Neurons and Muscles for Shell Continua, The 1991 ASME Design Technical Conferences – 13th Biennial Conference on Mechanical Vibration and Noise, Structural Vibration and Acoustics, 1991, Vol. 34, pp. 1÷6.

Tłumienie drgań poprzez tłumik drgań skrętnych podczas rozruchu układu napędowego

Streszczenie

Praca dotyczy badania tłumienia drgań nieliniowych układu mechanicznego o dwóch stopniach swobody zawierającego tłumik drgań skrętnych. Rozważany jest rozruch układu przy wymuszeniu harmonicznym z jednostajnie zmienną częstością o stałej amplitudzie momentu wymuszającego. Uwzględniono tłumienie drgań wykorzystując zjawisko tarcia konstrukcyjnego (tłumienie pasywne) i efekt piezoelektryczny (tłumienie aktywne).

Zagadnienie rozpatrywane jest przy założeniu równomiernego rozkładu nacisków jednostkowych występujących pomiędzy współpracującymi powierzchniami tarcz ciernych i bezwładnika. Zbadano wpływ przyspieszenia kątowego, nacisku jednostkowego, obciążenia zewnętrznego oraz współczynnika wzmocnienia na krzywe rezonansowe drgań rozruchowych. Równania ruchu badanego układu mechanicznego rozwiązano wykorzystując asymptotyczną metodę Kryłowa – Bogolubowa – Mitropolskiego i metodę symulacji cyfrowej.